Meteorological Applications

RMetS Royal Meteorological Society

RESEARCH ARTICLE OPEN ACCESS

Understanding and Anticipating Anomalous Surface Impacts During Large-Scale Regimes

Judith Gerighausen[1] | Joshua Oldham-Dorrington[1,2] | Fabian Mockert[1] | Marisol Osman[1,3] | Christian M. Grams[1,4]

[1]Department Troposphere Research, Institute of Meteorology and Climate Research (IMKTRO), Karlsruhe Institute of Technology (KIT), Karlsruhe, Germany | [2]Geophysical Institute, University of Bergen, Bergen, Norway | [3]Facultad de Ciencias Exactas y Naturales, Departamento de Ciencias de la Atmósfera y los Océanos, CONICET – Universidad de Buenos Aires, Centro de Investigaciones del Mar y la Atmósfera (CIMA), CNRS – IRD – CONICET – UBA, Instituto Franco-Argentino para el Estudio del Clima y sus Impactos (IRL 3351 IFAECI), Universidad de Buenos Aires, Buenos Aires, Argentina | [4]Federal Office of Meteorology and Climatology, MeteoSwiss, Zürich, Switzerland

Correspondence: Joshua Oldham-Dorrington (joshua.dorrington@uib.no)

Received: 2 October 2024 | **Revised:** 8 August 2025 | **Accepted:** 26 August 2025

Funding: This work was supported by Deutsche Forschungsgemeinschaft, SFB/TRR 165; Helmholtz Association, VH-NG-1243.

Keywords: energy meteorology | synoptic dynamics | weather regimes

ABSTRACT

Weather regimes describe the large-scale atmospheric circulation in the mid-latitudes in terms of a few circulation states that modulate regional surface weather conditions on time scales of multiple days to a few weeks. This low-dimensional representation of weather has proven useful for the study of large-scale dynamics, climate trends, flow-dependent predictability, and as proxies for applied medium- to extended-range forecasting in the energy sector, for example. Previous studies have often focused on the mean surface weather associated with a regime, with only a few commenting quantitatively on intra-regime variability. In this paper, we comprehensively quantify variability of daily surface weather within regimes and show that it cannot be ignored as mean-composite approaches can be misleading. Signal-to-noise metrics highlight regime configurations that provide windows of predictive opportunity, where surface dynamics are well controlled by the large-scale regime. We discuss in detail wintertime temperature and wind speed regime anomalies for four selected countries (Spain, Norway, Germany, and the United Kingdom) and show that in each case there is impactful intra-regime variability that can be explained by different subtypes and life cycle stages of a regime. This nuance can be captured by continuous regime indices, allowing a refined application of weather regimes on the pan-European scale. This relatively simple guidance on regime interpretation and operational use comes without the need to change the underlying regime framework. An accompanying interactive archive, documenting intra-regime variability in national-scale, energy-relevant variables, supports immediate practical application of our regime analysis for all European countries.

1 | Introduction

As a result of the chaotic nature of the atmosphere, the direct prediction of surface weather in Europe with any deterministic accuracy has long been limited to between 1 and 2 weeks (Buizza and Leutbecher 2015). However, demand from stakeholders—especially in the energy sector—for weather predictions on the subseasonal timescale (2–6 weeks) is growing, as accurate forecasts of temperature, wind, precipitation, and solar radiation anomalies help anticipate renewable output and power demand. Longer-range access to this information is vital for activities such as forward planning of grid and power plant maintenance, and can be highly profitable for traders on the energy futures market. Subseasonal forecasting for Europe is made feasible by the considerable structured, low-frequency variability of the Euro-Atlantic extratropical circulation, which

is often understood through the lens of weather regimes: categorical representations of recurrent quasi-stationary and persistent flow patterns (e.g., Reinhold and Pierrehumbert 1982; Vautard 1990; Michelangeli et al. 1995) that typically last several days to a few weeks. The regime concept emerged from initially theoretical considerations (Charney and DeVore 1979), and such regimes show signs of dynamically meaningful behavior (Faranda et al. 2016; Hochman et al. 2021), which helps explain their potential for extended-range predictability (see Hannachi et al. 2017, for an extended review). While exact definitions are diverse, common regime approaches typically capture the two phases of the North Atlantic Oscillation (NAO) and a small number of blocked and/or cyclonic states over the east Atlantic and western Europe (Vautard 1990; Ferranti et al. 2015).

As regimes modulate large-scale multi-day surface weather conditions and the occurrence of extremes (e.g., Yiou and Nogaj 2004), their potential value for skilful prediction beyond 2 weeks has been long recognized (Reinhold 1987) and has, to some extent, been realized (Ferranti et al. 2015; Matsueda and Palmer 2018; Büeler et al. 2021; Osman et al. 2023), proving useful for the energy sector (Van Der Wiel et al. 2019; Bloomfield et al. 2020). In recent years, awareness of the role meteorological variability plays in renewable power systems has risen (Zubiate et al. 2017; Grams et al. 2017; Van Der Wiel et al. 2019; Bloomfield et al. 2021; Mockert et al. 2023, e.g.). The regime concept has been extended to East Asia and South Asia (Matsueda and Kyouda 2016; Howard et al. 2022), and North America (Lee et al. 2019, 2023; Liu et al. 2023) and unified with the European perspective (Messori and Dorrington 2023), supporting regime perspectives on pan-Atlantic surface impacts.

Crucially, however, accurate regime predictions do not always result in accurate prediction of surface weather. For example, the state of the wintertime stratospheric polar vortex is known to modulate the occurrence of the different NAO phases (Baldwin et al. 2003). This generally provides a window of subseasonal forecast opportunity in the Northern Hemisphere, with enhanced skill for the large-scale circulation (Ferranti et al. 2015; Matsueda and Palmer 2018; Spaeth et al. 2024). However, a weak stratospheric polar vortex can result in reduced skill for surface temperature and other energy-relevant parameters in Europe (Büeler et al. 2020; Domeisen et al. 2020). For Greenland blocking, related to the negative NAO, Spaeth et al. (2024) recently explained this as a result of considerable uncertainty in surface temperatures even when the prevailing regime is known. With focus on renewable energies, Bloomfield et al. (2021) provide one of the few studies systematically comparing skill of regime approaches on subseasonal scales compared to grid-point based forecasts. While traditional regimes tend to have more skill beyond week 2 than targeted circulation types, the latter better represent the surface weather modulation relevant to the energy sector (see also Bloomfield et al. (2020)). Cautionary remarks on intra-regime variability, and the need to look beyond mean regime signals have been raised previously in the literature (e.g., Neal et al. 2016; Zubiate et al. 2017; Grams et al. 2017, 2020). Still, to our knowledge, a quantitative pan-European analysis of exactly how much intra-regime variability there is has not been shown, except in the context of the more regional circulation or weather types (Schiemann and Frei 2010).

The complementary perspective of daily weather patterns or types provides a more fine-grained perspective by using a much larger number of patterns than is typical in regime approaches. Historically, it has roots in the synoptic analysis of daily weather variability, dating back to the concept of "Grosswetterlagen" introduced by Hess and Brezowsky (1952, 1977), and has been greatly expanded upon, generalized, and synthesized across European regions since then (Tveito and Huth 2016). The hierarchical approach of Neal et al. (2016) permits a hybrid perspective, using 30 weather patterns suitable for short timescales and high characterization of daily surface impact, which is particularly suited for short-term forecasting up to about 7 days. It then aggregates into eight regimes with similar large-scale circulation characteristics in the North-Atlantic European region representing multiday variability, and particularly useful for medium- to extended-range forecasting > 1 week. This perspective has been developed into the hierarchical weather type/regime tool "Decider", implemented on multi-model forecasts by the UK Met Office (Neal et al. 2024), and has demonstrated utility for various applications, such as forecasting local extreme precipitation and potential flood conditions (Richardson et al. 2020), the risk of volcanic ash transport to the British Isles (Harrison et al. 2022), but also critical situations in the British energy sector (Souto et al. 2024).

In this study, we aim to show how the detailed variability of surface weather can be quantified while staying within the relatively simple framework of a small number of regimes. Specifically, we show how continuous regime indices can identify distinct subtypes of regimes with radically different surface impacts. Working within the 7 year-round regime framework of Grams et al. (2017), we present a detailed analysis of intra-regime variability in 2 m temperature (T2m) and 100 m wind speed anomalies (W100m) during the winter (DJF) season, when European energy demand is highest. The Supporting Information Gerighausen et al. (2024) provides a comprehensive catalogue of intra-regime variability for 3136 combinations of regime, season, variable, and region, which we here introduce through a small number of demonstrative examples. We highlight when and where intra-regime variability is and is not important and how, in many cases, it can be accounted for to distinguish between cold/calm and warm/windy anomalies in a given regime. We also provide a motivational case study of seamlessly predicting the surface impact for a prolonged regime event that showed dramatic variations in surface weather during its lifetime. Data and methods are described in Section 2, our results are discussed in Section 3, and we present our conclusions in Section 4.

2 | Data and Methods

2.1 | Weather Regime Definition and Characteristics

We use the ERA5 reanalysis from the European Centre for Medium-Range Weather Forecasts (Hersbach et al. 2020) over the 43-year period from 01/01/1979 to 31/12/2021. Seven year-round weather regimes are defined following Grams et al. (2017), based on EOF-analysis and *k*-means clustering of 10-day low-pass filtered 500 hPa geopotential height anomalies

(Z500′ with respect to a 1979–2019 climatological period) in the North-Atlantic European sector (80° W–40° E, 30° N–90° N), adapted to ERA5 as explained in Hauser, Teubler, et al. (2023).

Wintertime temperature and wind-speed anomalies during each weather regime are shown in Figures 1a–h and 2a–h, respectively. Broadly speaking, the seven regimes distinguish two main groups: the "cyclonic regimes", Atlantic Trough (AT), Zonal (ZO), and Scandinavian Trough (ScTr), which are characterized by cyclone activity in the North Atlantic European domain and, in winter, bring mild and windy conditions to wide parts of Europe (Figure 1a–c). The "anticyclonic regimes," Atlantic Ridge (AR), European Blocking (EuBL), Scandinavian Blocking (ScBL), and Greenland Blocking (GL), are characterized by a blocking anticyclone in the domain and bring calm but colder weather to Central Europe in winter (Figure 1d–g).

In the following we briefly discuss some more details based on the surface conditions in winter, but we refer to the more thorough discussion, including the typical Z500 anomalies in the supplement of Grams et al. (2017). The ZO regime corresponds to the positive phase of the NAO and features a strong Icelandic low and above average T2m in most regions of Europe (Figure 1b). At the same time ZO brings above average mean wind speeds to the UK and countries adjacent to the North and Baltic Seas (2b). Variants of these cyclonic regimes are AT and ScTr with cyclone

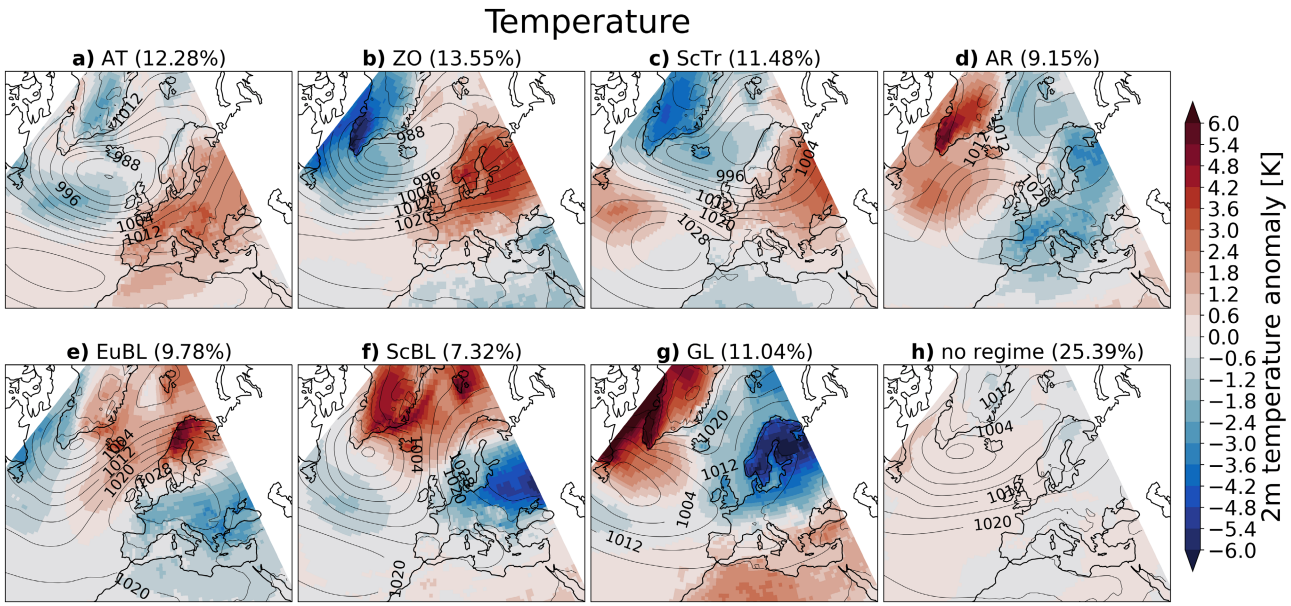

FIGURE 1 | T2m anomalies during DJF in (°C) for the seven weather regimes: (a) Atlantic Trough (AT), (b) Zonal (ZO), (c) Scandinavian Trough (ScTr), (d) Atlantic Ridge (AR), (e) European Blocking (EuBl), (f) Scandinavian Blocking (ScBl), (g) Greenland Blocking (GL), and (h) no regime. Black contours show mean sea level pressure (every 4 hPa). The occurrence frequency of each regime is given in brackets.

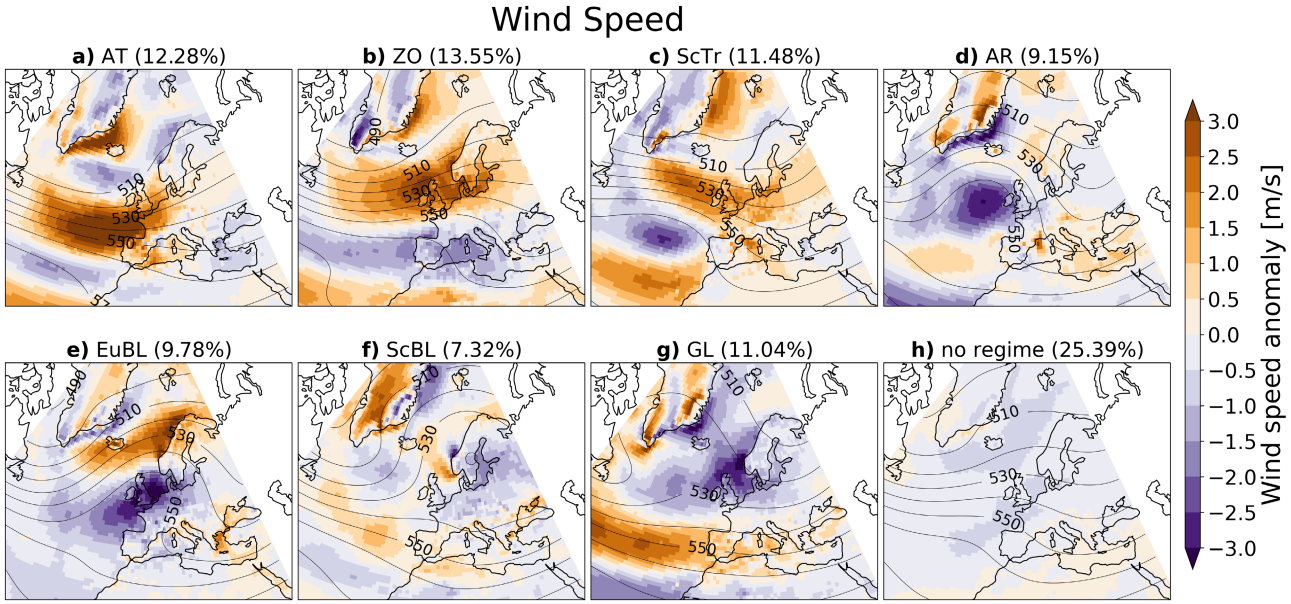

FIGURE 2 | DJF Wind anomalies in (m/s) for the seven weather regimes and the no regime in shading, as in Figure 1, together with 500 hPa geopotential height (black contours every 10 gpdm). The occurrence frequency of the regimes is given in brackets.

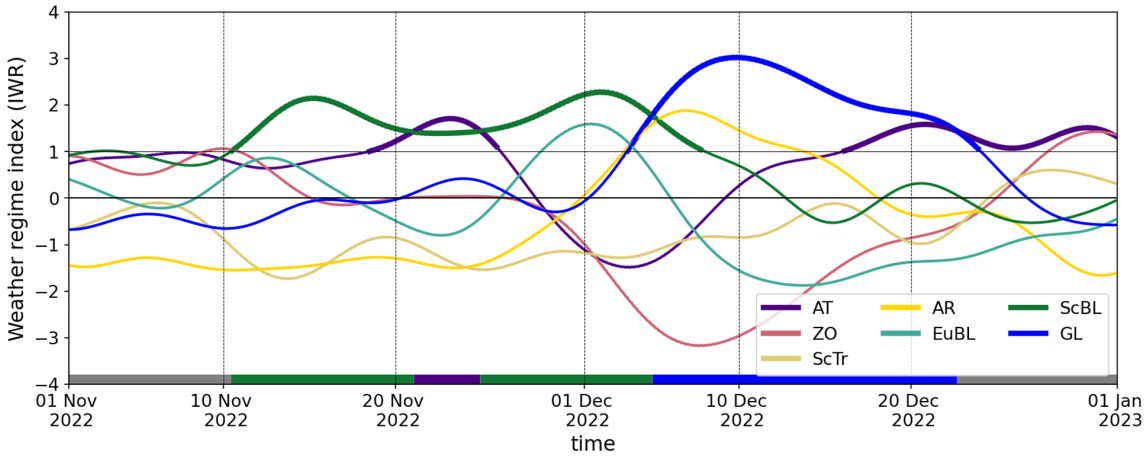

FIGURE 3 | Time series of I_{wr} in November and December 2022. Each colored line shows the normalized weather regime index I_{wr} for one of the regimes in units of one standard deviation (y-axis). Bold lines show active regime life cycles defined as in Hauser, Teubler, et al. (2023). The bar at the bottom indicates the categorical attribution of the dominant active life cycle with grey indicating "no regime" days. Data is based on 3-hourly ERA5 reanalysis.

activity shifted toward western Europe or Scandinavia, respectively, and corresponding shifts in the patterns of T2m and wind speed anomalies (Figures 1a,c and 2a,c). Importantly ScTr is accompanied by a weak ridge (in Z500, Figure 2c) over the Atlantic. The related AR regime features a much more amplified ridge and a blocking high pressure systems resides over the eastern North Atlantic and western Europe, with only weaker cyclone activity in Northern Scandinavia (Figures 1d and 2d). Almost all of Europe experiences below average T2m and windspeed. In southeastern Europe, the central and eastern Mediterranean as well as part of Scandinavia wind speed is enhanced during AR. Other anticyclonic regimes over Europe are EuBL and ScBL, with a blocking high pressure system over central and Northeastern Europe, respectively, and accompanying cold conditions over most of Europe, except for parts of Scandinavia (Figure 1e,f). Also windspeeds are reduced in the North and Baltic Seas region during EuBL and ScBL, while peripheral regions of Europe experience above average wind speed (Figure 2e,f). Finally, GL corresponds to the negative phase of the NAO, with a blocking high pressure system over Greenland and very cold conditions in Northern Europe, while the Mediterranean is milder, in particular Iberia (Figure 1g). Also wind speed is below average in most of Europe, except for enhanced windspeed in Iberia and the Mediterranean (Figure 2g). Days attributed to none of the seven regimes ("no regime" days) discern hardly from climatology (Figures 1h and 2h).

The weather regime index, I_{wr}, serves as a continuous measure of weather regime activity and is defined as the normalized projection of 3-hourly Z500′ onto each of the seven cluster means. As well as being useful for characterizing North-Atlantic European flow variability, the I_{wr} also permits the definition of discrete active life cycles for each regime. Concretely, a regime, R, is considered active if $I_{wr=R} > 1.0$ for at least five consecutive days (see Hauser, Teubler, et al. 2023, for details). If no regime meets this criterion for a given date, that date is categorized as "no regime", following (Grams et al. 2017).

We illustrate the concept of I_{wr} with an example for November and December 2022, which will also serve as a case study later. Figure 3 shows the I_{wr} for all seven regimes. Around 10 November I_{ScBL} (dark green) strongly increases, indicating the begin of a regime life cycle that lasts until 8 December when I_{ScBL} falls below 1.0. A peculiarity of the regime definition of Grams et al. (2017) is that it allows life cycles being active at the same time, which other studies showed is physically meaningful. This happens from 18 to 26 November, when I_{AT} (violet) is above 1.0 and becomes the dominant regime from 21 to 25 November (bar at the bottom of Figure 3). This co-existence of life cycles means, that blocking persists over Scandinavia but is accompanied intermittently for a couple of days by a strong upstream trough, which projects into AT (cf. contours of Z500 in Figure 1a,f). In early December the ScBL life cycle transitions into a GL regime, reflected in a gradual decay of I_{ScBL} and an increase in I_{GL} (blue). The GL life cycle starts on 3 December and becomes the dominant regime on 5 December. In the first half of the GL life cycle the I_{AR} (yellow) is also high, but later an incipient AT (violet) life cycle becomes a secondary regime. We come back to this important aspect of secondary regime activity later in this paper.

2.2 | Surface Weather Anomalies

Daily mean anomalies (computed from 6-hourly ERA5 data) of 2-m temperature (T2m) and 100-m wind speed (W100m) are computed with respect to the 31-day running mean climatology at a given calendar day (1979–2021) using data on a 1° grid. Then, a linear day-of-year trend is removed to account for any potential climate change impact, and a five-day rolling mean is applied to remove sub-synoptic variability.

The surface weather anomalies are spatially-averaged over the national boundaries of European countries (masked with Python-package "regionmask", available from https://github.com/regionmask/regionmask), using cosine-latitude weighting, to yield scalar time-series of country-aggregated weather. These time series are stratified into terciles for a given regime and season to investigate differences between cold/calm and warm/windy situations. After stratification into terciles, we consider

the averaged temporal evolution of all seven I_{wr} indices in a 20-day window centred on each date in the respective tercile. The resulting lagged I_{wr} composites allow us to see if the upper or lower tercile days systematically occur in a late or early stage of a regime's life cycle, or if other regimes are simultaneously active. Significant differences in intra-regime flow evolution are quantified with a Kolmogorov–Smirnov test (Stephens 1974) at the 1% level between I_{wr} indices in the tercile of interest and those in the other two terciles at each time step. As a sensitivity test for any impacts of autocorrelation we repeated our analysis stratifying by independent extreme events, and found qualitatively similar results. Concretely, Figures S1 and S2 show equivalent results to Figures 7 and 8, but stratified by the 10 most extreme days coming from individual, separate regime life cycles. The 10 events are therefore temporally well separated and temporal autocorrelation is excluded by construction.

2.3 | Metrics

To analyse how surface weather anomalies vary within days belonging to a given regime, we define two gridpoint metrics: the fractional standard deviation (FSTD), $\sigma_{\text{frac,season}}$:

$$\sigma_{\text{frac,season}} = \frac{\sigma_{\text{regime,season}}}{\sigma_{\text{season}}} \tag{1}$$

and the signal-to-noise ratio (S2N):

$$\text{S2N} = \left| \frac{X_{\text{regime,season}}}{\sigma_{\text{season}}} \right| \tag{2}$$

where X stands for the T2m or W100m anomaly.

These metrics simply correspond to the standard deviation and the (sign-invariant) mean of surface weather anomalies in a regime, respectively, scaled by the seasonal standard deviation of surface weather. Values of FSTD < 1 indicate a reduction in surface-weather variability within a regime compared to the season as a whole, with FSTD $= 0$ corresponding to the naive perspective that *all* surface weather is accounted for by regime activity. Conversely, FSTD > 1 indicates increased surface weather uncertainty within a given regime, due to sensitivity to small-changes in the large-scale flow. High S2N, meanwhile, indicates that surface weather anomalies are meaningfully strong compared to climatic variability. If S2N is low, then the net shift in surface weather is negligible in comparison to variability. Importantly however, low S2N does not necessarily imply no impact of the given regime on surface weather. This is only the case if FSTD is close to 1.

3 | Results

3.1 | Modulation of Surface Weather Variability by Weather Regimes in Winter

A main motivation of this paper is to shed light on how much weather regimes affect the daily surface weather variability in different regions, in addition to the shift in mean conditions summarized in Section 2.1. Therefore, we start with a discussion of the modulation of surface weather variability during regimes in winter in terms of our two metrics FSTD and S2N, shown in DJF for each regime in Figures 4a–p and 5a–p, respectively.

In general, DJF T2m and wind variability is reduced within a given regime compared to climatology (i.e., FSTD < 1), supporting the practical utility of regimes for modulating surface weather (Figure 4). For T2m the notable exceptions are Mediterranean temperatures during AR (Figure 4d), and—particularly clearly—south-west European temperatures during GL (Figure 4g), which both show elevated temperature variability. For GL, this region of unconstrained temperatures is co-located with a southward-shifted jet and the eastern edge of a surface cyclone in the composite mean (c.f. Z500 contours and MSLP contours in Figure 4g,o, respectively), reflecting the southward shift of the storm track during GL (cf. Hauser, Mueller, et al. 2023). In this region, mean temperature anomalies are weak (Figure 1g) and S2N is low (cyan contour in Figures 4g and 5g): there is little mean effect of GL on southwest European temperature. It is only over Northern Europe where FSTD < 1 and S2N > 1, indicating reliably and robustly colder weather than usual during GL. Elsewhere the impact of GL is uncertain, a result of the dominant anticyclonic anomaly that defines the regime sitting far upstream and to the north of Europe.

Intra-regime W100m variability is comparatively more heterogeneous (Figure 4i–p). Areas of high S2N are rare and spatially localized. Importantly, during AT and ZO, high S2N together with low FSTD occur over the western coasts of Europe and the North Sea (Figure 4i,j), respectively, colocated with robust positive W100m anomaly during AT and ZO (cf. Figures 2a,b and 5i,j), which has relevance for regional wind power production (cf. Grams et al. 2017). These areas with low FSTD and high S2N indicate regime configurations that provide potential windows of predictive opportunity, where surface dynamics are well controlled by the large-scale regime. Overall, during all zonal regimes (AT, ZO, ScTr) intra-regime variability along western and northern European coasts is reduced (Figure 4i–k). However, further inland, variability is also enhanced while S2N is generally low (Figures 2a–c and 5i–k). During blocked regimes (AR, EuBL, ScBL, GL), wind speed varies less directly under the anticyclone (AR, EuBL, ScBL, Figures 2d–f and 4l–n) or in the case of GL (Figures 2g and 4o) at the eastern flank of the accompanying upper-level ridge and surface high (contours in Figures 2a–c and 4l–o). As for the zonal regimes, local areas can see enhanced intra-regime variability, such as the Alps and parts of Scandinavia and eastern Europe for AR, EuBL, and ScBL. GL sees enhanced wind speed variability over the North Atlantic and southern Spain. Notably, a high S2N over the North Sea region in EuBL and GL indicates robust calm conditions (cf. Figures 2e,g and 5m,o) in alignment with Grams et al. (cf. 2017); Mockert et al. (cf. 2023).

3.2 | Details on Intra-Regime Temperature Variability

More insights into intra-regime variability in specific regions can be gained from probability distributions of country-aggregated surface weather anomalies within each regime, shown in Figure 6a–d. As a first example, we discuss intra-regime T2m

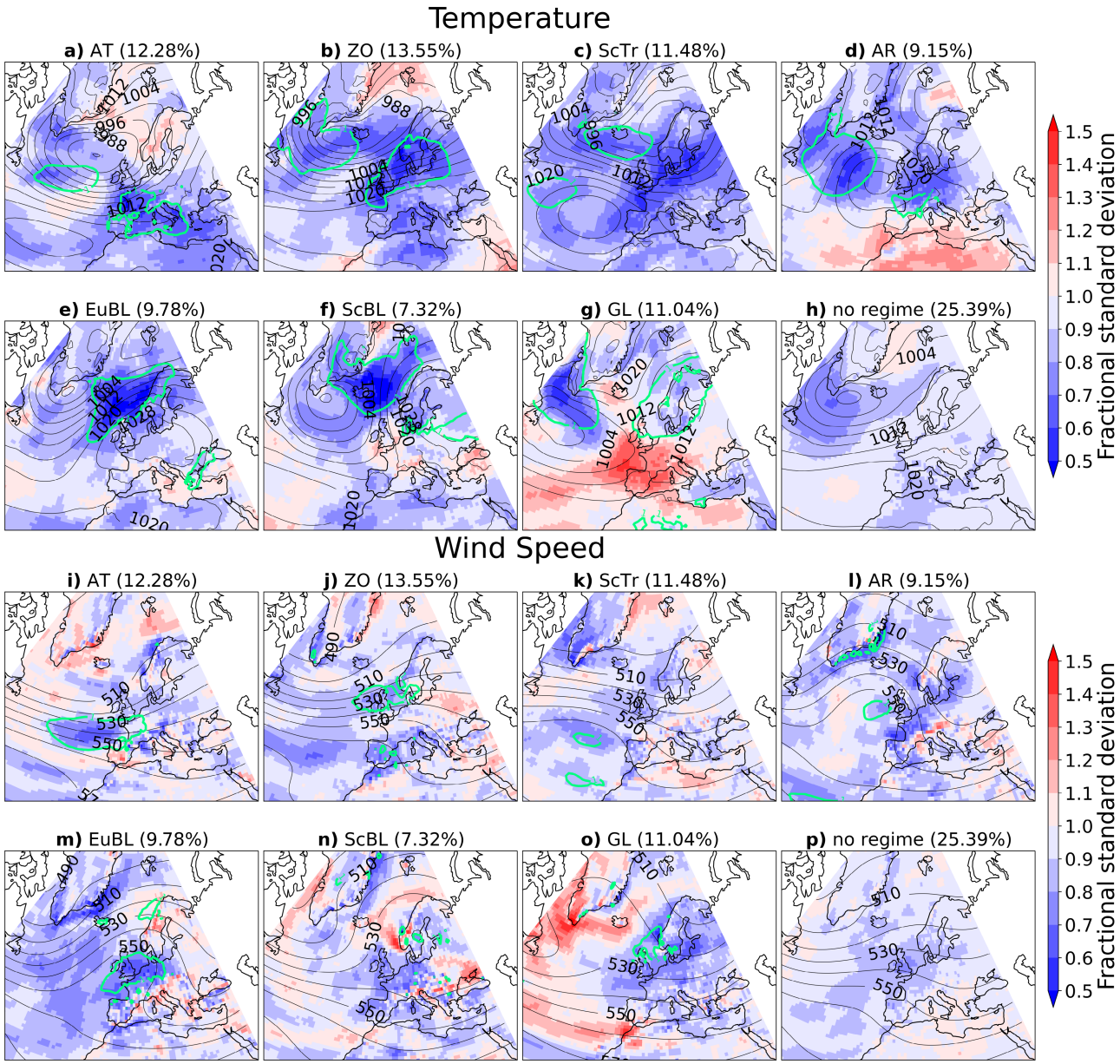

FIGURE 4 | (a–h) Fractional standard deviation (FSTD) of 2 m wintertime temperature regime anomalies with mean sea level pressure overlaid (contours every 4 hPa). (i–p) FSTD of 100 m wind speed anomalies with 500 hPa geopotential height overlaid (contours every 10 gpdm). Cyan contours indicate areas with signal to noise ratio > 1 (cf. Figure 5). Percentages above each panel indicate wintertime regime occurrence frequency.

variability for Spain and Norway to shed light on the marked FSTD pattern for GL discussed in the previous section. Wintertime temperature variability in Spain is largest during GL spanning a range of approximately 14 K (c.f. Figure 6a); comparable to the total climatology. With a median temperature anomaly of approximately 1 K, GL is in fact the second warmest regime in Spain on average, but features a long tail of cold anomalies. As such, the coldest anomalies during GL, approximately 6 K below typical conditions, are only surpassed by the coldest AR and EuBL events. This non-negligible probability of cold anomalies is remarkable and totally missing from the mean picture of GL as mild in Iberia. This could easily lead to false forecasting assumptions. In contrast, GL brings reliably cold weather to Norway in winter, almost always colder than typical and with a median temperature anomaly of approximately −4 K (Figure 6b). Thus, the variability of GL in this region is one of *degree*; whether a GL regime bring cold or extremely cold conditions.

In order to give guidance in these two contrasting cases of Spain and Norway, we explore differences in the atmospheric flow pattern for GL days in the upper and lower tercile of T2m anomalies (Figure 7a–f), and in lagged I_{wr} composites (Figure 7g–j). When GL brings cold anomalies over the Iberian Peninsula (Figure 7a), the ridge is shifted east over the Atlantic Ocean compared to average GL days (Figure 7b), and the trough reaches from Scandinavia deep into Central Europe (Figure 7a). The jet stream shifts south over northern Africa and negative T2m anomalies extend over almost all of Europe. The I_{wr} composites (Figure 7g) reveal that the cold GL days in Spain occur around the peak of GL life cycles and tend to be embedded in longer but not necessarily stronger (in terms of I_{wr}) GL life

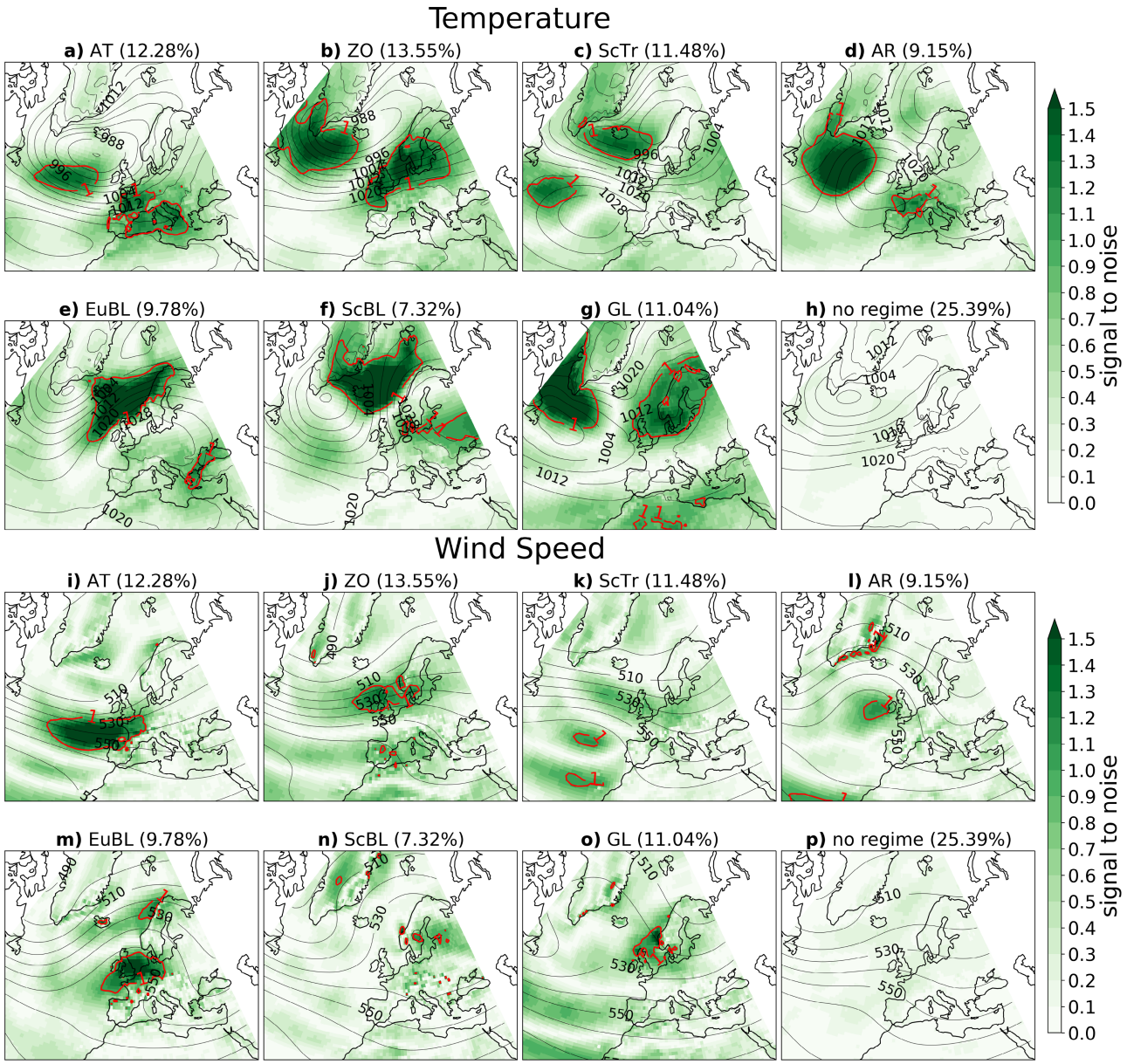

FIGURE 5 | (a–h) Absolute values of the signal to noise ratio of T2m anomalies during the seven weather regimes and the no regime in shadings during DJF over Europe and the North Atlantic with mean sea level pressure (black contours every 4 hPa). The red line indicates values above 1. (i–p) Absolute values of the signal to noise ratio of wind speed anomalies during the seven weather regimes and the no regime in shadings during DJF over Europe and the North Atlantic together with 500 hPa geopotential height (black contours every 10 gpdm). The red line indicates values above 1.

cycles. More relevant in explaining contrasting T2m anomalies during GL in Spain is the co-projection into a secondary regime, namely AR, about 3 days prior to the coldest GL days in Spain. AR I_{wr} first exceeds 1 at day −6, shortly after the GL I_{wr} exceeded 1 and decays around the peak of GL at day +2. At the same time there is a strong anti-projection into ZO. The co-occurring AR and strongly suppressed ZO reflects exactly the eastward shifted and intensified ridge-trough setup, supporting cold air advection from the North and Northeast into the continent. Warm GL days in Spain occur when the ridge over the Atlantic has a northwestern-southeastern tilt, and the jet is wavier (Figure 7c). The flow pattern over the western Mediterranean is more south-westerly, leading to warm air advection, while the cold air remains confined over Scandinavia and eastern Europe (Figure 7c). This occurs shortly after the peak of GL together with an anomalous co-projection in AT, while the signature of the other anticyclonic regimes is weaker (Figure 7h). Thus for GL days in Spain a co-projection in AR results in cold anomalies, whereas AT co-projection results in warm anomalies. A similar behavior is observed for Western and Central European countries such as Germany (see Supporting Information). In particular for Germany, a co-projection in AR or AT modulates the potential for energy-critical cold and calm conditions during GL (Mockert et al. 2023).

For Norway, cold days during GL show a ridge shifted westward (c.f. Figure 7d,e), over the North Atlantic and Greenland. The trough over Scandinavia is more extensive than average, bringing extremely cold anomalies to the whole region. Adjacent regions, such as the British Isles or Poland, also experience colder

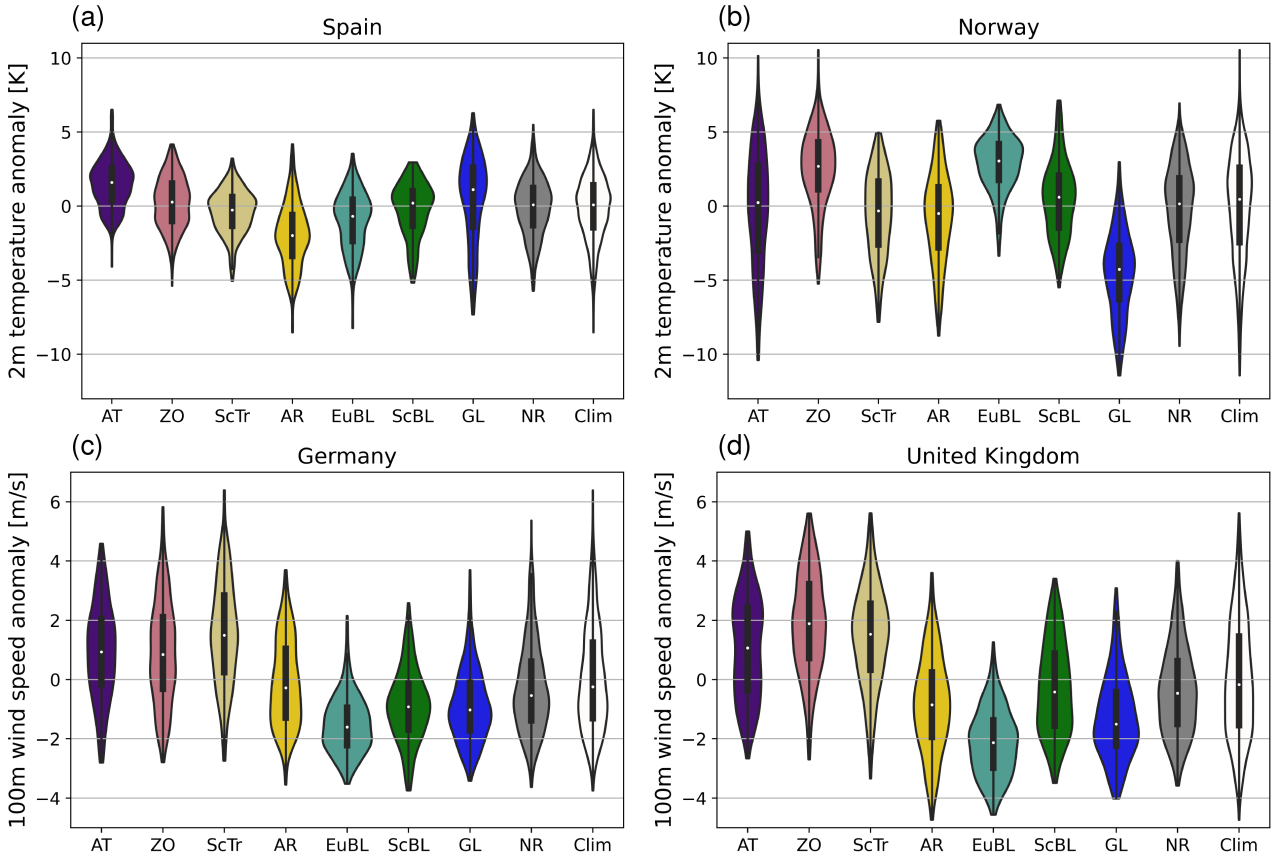

FIGURE 6 | Distributions of daily 2—metre temperature anomalies (T2m) in Spain and Norway (a, b) and 100—metre wind speed anomalies (W100m) in Germany and the United Kingdom (c, d) for all days in each regime, no regime and the wintertime climatology. Black boxes within each distribution indicate the interquartile range, while white dots mark the median of each distribution.

anomalies from the stronger intrusion of polar air. Southern Europe experiences modestly strengthened warm anomalies, and so temperature gradients over central Europe are intensified. Relatedly, the jet stream is shifted south and intensified over the Mediterranean (contours of 500 hPa geopotential height in Figure 7d).

These flow changes again project well onto the I_{wr} (Figure 7i). From a secondary regime perspective there is a relatively strong co-projection into AR prior to cold days, and into AT during the coldest days, while other regimes are suppressed (Figure 7i). Cold GL days in Norway are on average 2 days longer than the moderately cold GL days (in terms of period with mean $I_{wr} > 1.0$) and the coldest days (lag 0) generally occur in the decaying stages of the regime, with peak GL I_{wr} 3–4 days prior and higher amplitude than in the other terciles. This suggests a clear interpretation where the deep trough over Scandinavia, together with the ridge over Greenland leads to stronger northerly advection into Scandinavia, which builds to a peak during the final days of a long-lived GL life cycle (Bieli et al. 2015).

During upper-tercile T2m GL days over Norway, the anomalies are still cold, but mildly so, and spread over large parts of north and central Europe (Figure 7f). The ridge over the Atlantic is more pronounced and much more west–east tilted than on average, while the trough over Scandinavia is weaker. These days occur in the early stages of GL life cycles, about 2 days prior to the maximum mean I_{wr}, indicating that the GL life cycle is still in the developing phase (Figure 7j). Interestingly, a co-projection into ScBL and AR occurs before and around these least cold GL days in Norway, and co-projection into AT evolves only later. Thus monitoring the projection in AR, ScBL, and AT can help to assess the degree of cold response to GL in Norway. This analysis of cold and mild regime days may feature some confounding autocorrelation in the composite, as may the mean composite perspective over all days within a regime. However, this is intended as we aim to deduce the statistically significant differences in the subsets compared to all days. Nevertheless to further corroborate our findings we have repeated the analysis in an event-centric perspective (Figure S1). Here we select only the 10 most extreme days in terms of temperature anomalies and impose the requirement that these days must be chosen from individual, separate life cycles. In this event-centric perspective our key spatial and index-based findings still hold.

In summary, variations in the atmospheric flow pattern, that nevertheless project into the GL regime, are able to explain the variability of temperature anomalies over different countries. These changes project differently into the I_{wr} of the active, secondary, and suppressed regimes and reveal that in some cases, for example Norway, the anomalies depend strongly on the stage of the regime (early or late), while, for example, in Spain, co-occurring secondary regimes are of more importance. This knowledge can be used in weather forecasting by not only

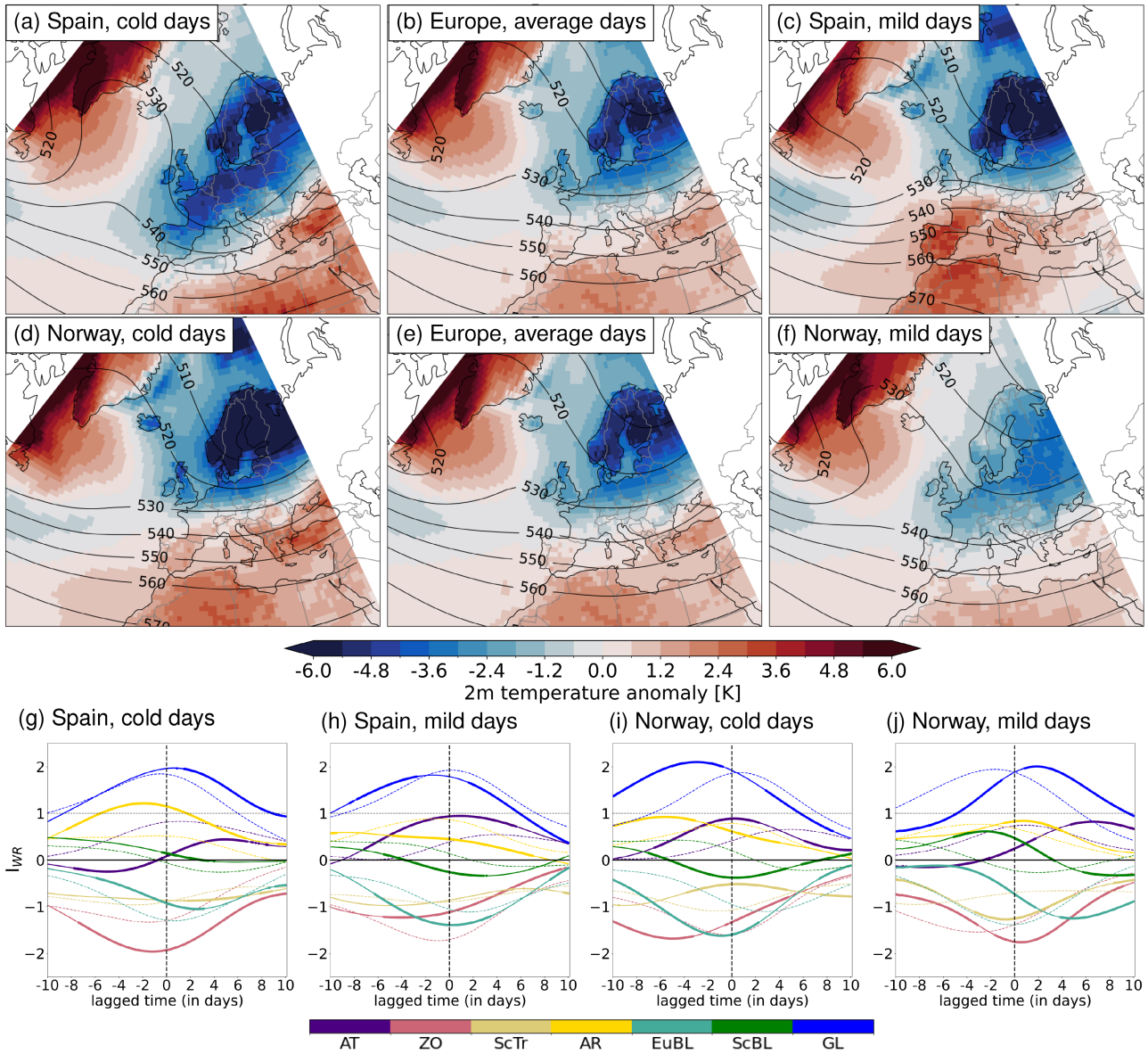

FIGURE 7 | Panels (a–f) Composites of wintertime 2 m temperature anomalies with absolute geopotential height composites overlaid for Greenland Blocking (GL) days in the lower (a, d—cold days) and upper tercile (c, f—warm days) in Spain (a, c) and in Norway (d, f). Composites for all wintertime GL days are displayed in b and e. Panels (g–j) Lagged composites of the I_{wr} index in a 20-day window centered on the date of lower/upper tercile day (lag = 0 days) in both countries shown as solid lines. Significant differences at 1% level between the lagged composite of I_{wr} for the tercile of interest and the lagged composite of I_{wr} for all other dates using a Kolmogorov–Smirnov test. Dashed lines show the lagged composite of I_{wr} for all other dates.

monitoring the potential most likely regime, but also the subtype of the current regime as captured by I_{wr} co-projections.

3.3 | Wind Speed Variability

As a next example we discuss the variability in W100m anomalies in Germany and the UK, shown for selected cases in Figure 8a–j. The distributions of W100m anomalies (Figure 6c,d) show that ScTr and ZO are the windiest regimes for Germany and the UK, respectively. Nevertheless, cyclonic intra-regime variability is clearly large, and even these windiest regimes can produce wind anomalies below −2 m/s. The large range of variability, with 25% of days actually calmer than average during cyclonic regimes, could lead to unexpected shortfalls in wind power output. The anticyclonic regimes are much less variable, especially EuBL, which brings calm conditions to both countries in almost all cases. AR in Germany and ScBL in the UK are calm on average as well but can bring windy conditions almost half the time. As the intra-regime variability of W100m is rather similar for Germany and UK, we focus on the anticyclonic AR regime for Germany and the cyclonic ZO regime for UK in the following. However, we note that results hold qualitatively for both countries (see Gerighausen et al. (2024)).

During calm AR days in Germany, the ridge over the North Atlantic extends further to the east and tilts in the southwest-northeast direction compared to average days (Figure 8a,b),

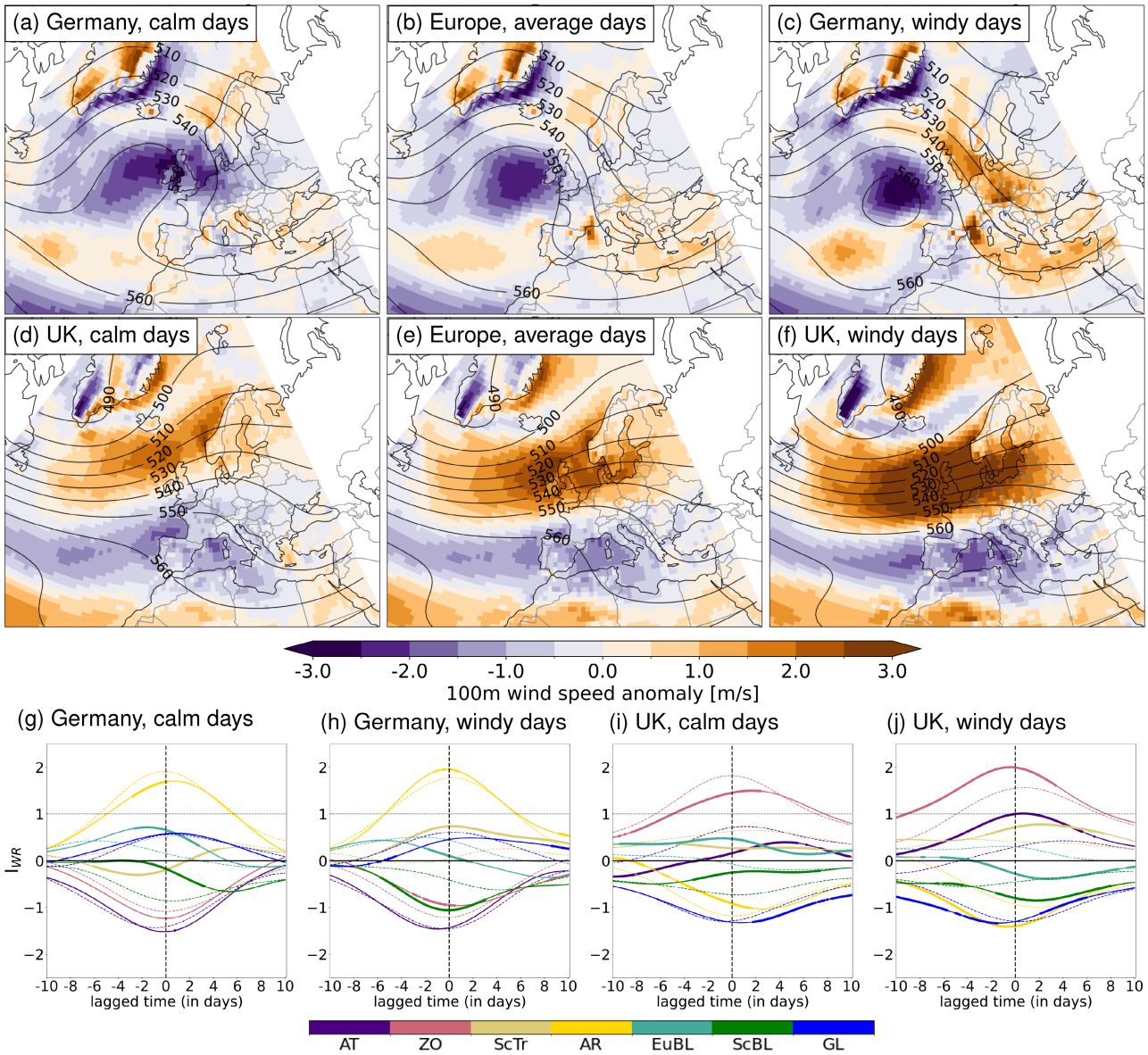

FIGURE 8 | As in Figure 7 but now for terciles of 100 m wind speed anomalies in Germany during Atlantic Ridge life cycles (a, c, g, h), and the UK during ZO life cycles (d, f, i, j).

indicative of anticyclonic wave breaking. This places Germany in a region of diffluent flow at 500 hPa where the reduced geopotential height (and mean sea level pressure) gradients likely explain below average W100m anomalies. The I_{wr} of AR is slightly but significantly weaker than on average just prior to peak (Figure 8g), but more important in this case are the secondary co-projections showing increased EuBL-I_{wr} and decreased ScTr-I_{wr}, which collectively capture the signature of the zonally extended ridge. By contrast, exceptionally windy AR days in Germany feature a strong ridge over the North Atlantic with an average geopotential height anomaly of 560 gpdm (Figure 8c), and a concomitant trough over Scandinavia. The resulting strong pressure gradient over the North Sea induces very windy conditions over Germany. I_{wr} for AR peaks around the windy days (Figure 8h), with a strong positive ScTr co-projection. Together, this places ScTr as the single most important secondary regime during AR events, which modulates the flow away from the dominating ridge, and so shapes the German wind impact. For the coastal climate of the UK, lying under the Atlantic storm track, the windiest ZO days occur during long, particularly strong ZO events (Figure 8e,f,j) with significant co-projection into the other cyclonic regimes. This leads to an intense, narrowed jet which extends eastward to Germany and the Baltics. Calm ZO days for the UK are a result of a northward jet excursion, for which the ZO-I_{wr} is below average, co-projections into other cyclonic regimes are reduced, while I_{wr} for EuBL is significantly enhanced (Figure 8d,i). Thus, a strong simultaneous projection on all cyclonic regimes captures abnormally strong wind impacts for the zonal regime, while an active EuBL projection can serve to deflect the jet enough to leave the UK calmed.

These two examples show that wind speed anomalies are just as impacted by regime internal variability as temperature anomalies

and can contain atypical impacts of opposite sign to the mean picture. This has clear implications for the wind energy sector. As for the temperature anomalies, we show how analysis of secondary regimes can shed light on these anomalous situations (AR regime in Germany), and indeed we find this is quite generally the case across countries, variables, and seasons (see the Supporting Information for a comprehensive catalogue of such signatures). We also see that in some cases the change of strength of the main regime itself can capture the majority of variability, as here for the UK under the ZO regime. As for the T2m example, our key findings hold also in the event-centric perspective focusing only on the 10 calmest or windiest days (Figure S2).

3.4 | An Exemplary Case Study

3.4.1 | Overview 2-m Temperature Modulation by GL in Germany in Winter

To illustrate the applicability of the proposed regime interpretation, we begin by introducing the interactive navigation panel accompanying the catalogue of additional plots downloadable as accompanying Supporting Information (Figure 9). The navigation panel eases users to explore the range of surface impacts within weather regimes across countries and seasons provided as plot collection: here exemplarily shown for DJF

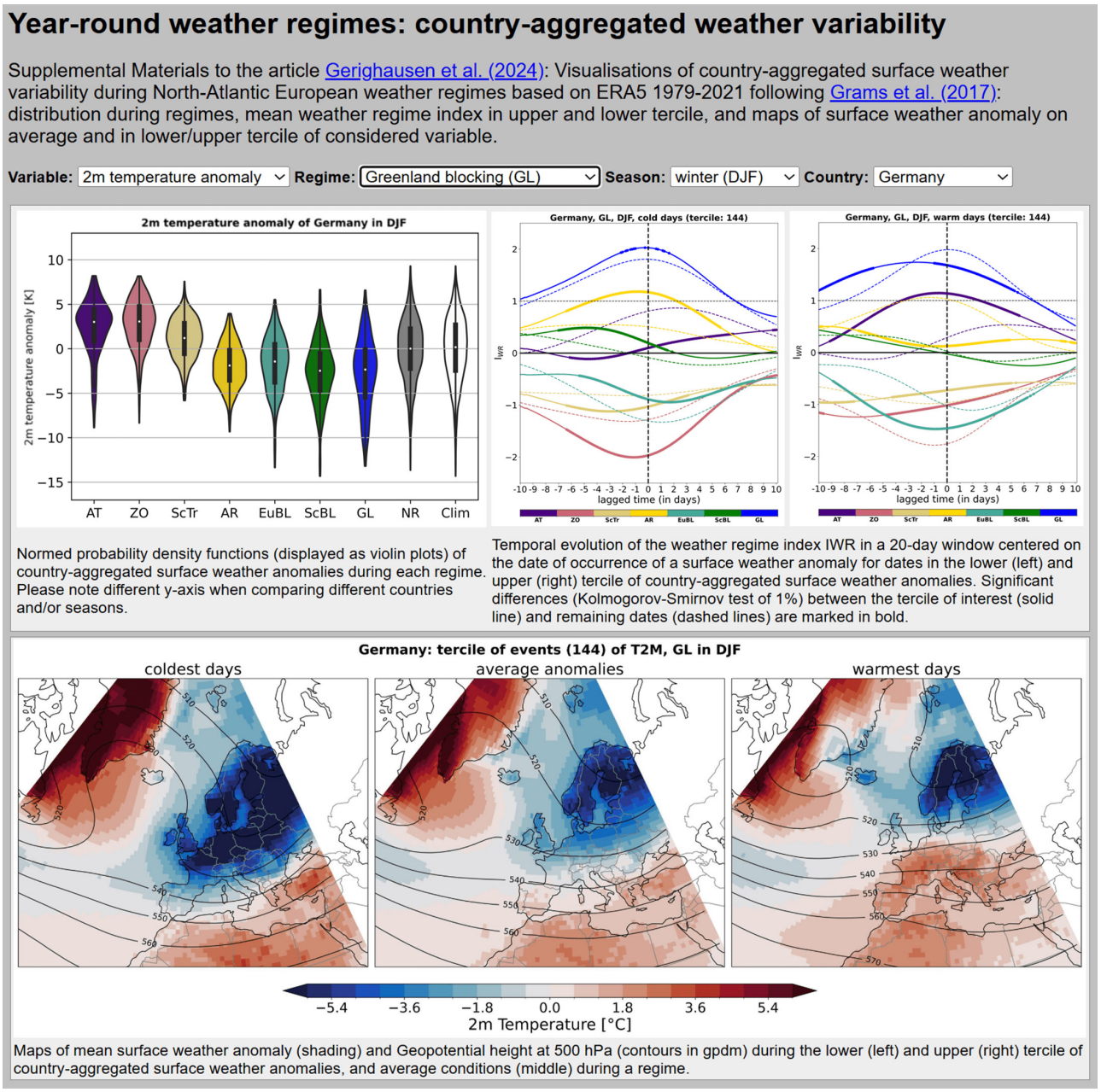

FIGURE 9 | Output from the interactive navigation panel showing 2-m temperature anomalies (T2m) during Greenland Blocking (GL) life cycles in Germany in winter (DJF): Distribution of daily country-averaged T2m anomalies on each winter day and for each regime (top left) as in Figure 6, and, as in Figure 7, lagged composites of the I_{wr} during cold GL (lower tercile, top middle) and warm GL days (upper tercile, top right figure), and composites of the T2m anomalies and geopotential height during cold GL (lower tercile, bottom left) and warm GL days (upper tercile, bottom right) are shown alongside average GL condition in winter (bottom middle).

GL impacts in Germany. The overview of country-aggregated surface weather anomalies for all regimes in the top left panel shows that GL brings cold T2m anomalies (< 0°C) to Germany 75% of the time. The middle and right panel on the top show that for cold GL days (lower tercile), the I_{wr} index for GL and (negative) I_{wr} index for ZO increase sharply in amplitude before day 0 and remain elevated afterward. With AR also active (reflected in high values of I_{wr} index for AR) this captures a large-scale Omega block over the North Atlantic, seen in the lower left panel. In contrast, warm GL days (upper tercile) typically occur during the decay phase of a weak GL regime (decreasing I_{wr} index for GL in upper right panel), and a concurrent increase in the AT regime, reflecting the isolation of the block westward and cyclonic conditions over Europe, which can be verified in the lower right panel. Equivalent information is provided for 26 European regions, in all seasons and for four key energy variables.

3.4.2 | The Case of December 2022

To further illustrate the practical value of the regime interpretation in a forecasting context, we present a short case study of a GL event during December 2022. Figure 10 shows the evolution of the continuous regime indices from ERA5 reanalysis and from the ECMWF IFS extended-range ensemble forecast, initialized at 00 UTC 28 November 2022 (7 days before GL onset). We also show the corresponding evolution of spatially averaged T2m in Germany and national onshore wind capacity factor (CF; a measure of theoretical renewable wind power; see Mockert et al. (2023) for computational details). In the early stages of the event, ERA5 and the forecast show a dominant ScBL life cycle with co-projection onto EuBL then a transition to GL with co-projection into AR (cf. discussion of Figure 3 in Section 2.1). As time progresses, both the observed and predicted signals transition toward a dominant GL regime in mid-December. Toward the end of the period, the GL signal weakens in both ERA5 and the forecast, while the projection onto AT strengthens only in ERA5, indicating a shift in the large-scale flow in the reanalysis that it is not well captured by the forecast. This evolution in regime projections (depicted by the I_{wr}) closely corresponds with surface impacts. As shown above, GL cold impacts are greatest during strong GL conditions accompanied by high projection on AR and suppression of ZO. As the flow transitions to AT, temperature recovers consistent with the climatological picture that mild GL days go along with an AT co-projection (Figure 9). Likewise wind power generation rises, as reflected by the increase in CF. These consistent relations between regimes and surface variables highlight the potential of the proposed

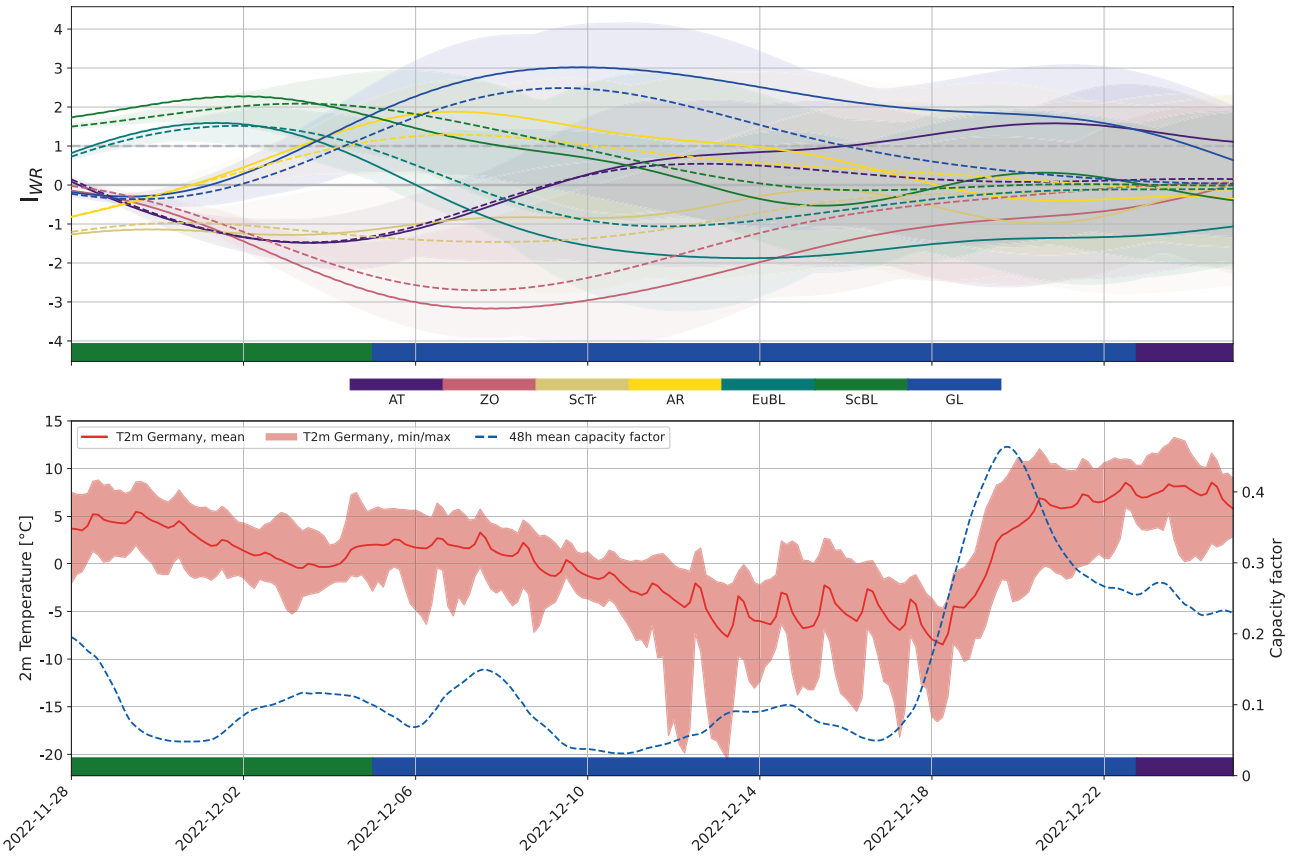

FIGURE 10 | Case study of a representative GL event in December 2022: Top: The solid lines show the actual evolution of the I_{wr} index for all regimes in ERA5 reanalysis. Dashed line shows the evolution in the ensemble mean of ECMWF IFS extended-range forecast initialized at 00 UTC 28 November 2022 and shading indicating the ensemble spread in terms of ±1 standard deviation amongst the 51 ensemble members. Bottom: Evolution of spatial mean T2m over Germany (solid red line), along with maximum and minimum values (red shading) taken from ERA5, and the onshore wind capacity factor in Germany (dashed blue line) computed as in Mockert et al. (2023). Temperature values are in °C. Data are shown for 4 weeks from 28 November to 25 December 2022 with 6-hourly time steps. The bar at the bottom of both plots indicates the maximum I_{wr}.

regime interpretation to inform possible impacts on temperature and renewable energy indicators. Importantly, this case study illustrates key aspects of regime evolution which can be monitored operationally and their surface impact. Although thorough verification is needed across a larger sample of events, I_{wr} indices are already known to be well forecast up to week 3 (Büeler et al. 2021). Future work developing the prediction strategy we suggest here should focus on attempting to boost usable skill in week 3 and extend into week 4.

4 | Conclusions

In this paper, we have presented a detailed quantitative analysis of internal variability of daily surface weather within North Atlantic–European weather regimes and provided a clear strategy for how to explain and account for that variability consistently within the underlying regime framework.

With four different examples, we have quantified and made explicit the earlier observation that variations in daily surface weather within a particular regime can be, and often are, large, and so should not be ignored in applications. This is somewhat intrinsic to the concept of weather regimes, which are mostly defined to capture low-frequency that is multi-day, variability of the large-scale circulation, and represent the most common quasi-stationary, persistent, and recurrent flow patterns. However, this notion strongly depends upon the European country considered with different characteristics of intra-regime variability in different sub-regions. At the same time, we show evidence that much of this intra-regime variability can still be understood within the underlying weather regime framework with the added aid of the continuous I_{wr} indices. As such, we provide a roadmap to more refined uses of weather regimes and interpretation of regime information which allow a user to choose an acceptable trade-off between complexity and discriminatory power. The application of this regime interpretation in a forecast context can be useful to anticipate impacts on surface variables, especially at longer leadtimes (beyond 7 days), when the skill of grid-point-based forecasts is reduced (Bloomfield et al. 2021). In forecasts situations where a predicted regime shows a high co-projection on another regime, users can confront this configuration of I_{wr} indices with the climatological regime information provided as Supporting Information and a prototype interactive navigation panel to anticipate the surface impacts that a particular country could experience.

Three main factors by which the regime indices I_{wr} modify surface weather are identified:

1. Secondary regime indices can be anomalously high, indicating a 'hybrid' regime,
2. The primary I_{wr} index may indicate that the surface anomalies preferentially occur early/late in a regime's life cycle,
3. The magnitude of the primary I_{wr} index itself may be exceptionally strong or weak.

Often a combination of at least two factors is evident. Rare cases do exist, where either no projection into the I_{wr} is significant and/or there are no changes in the flow pattern, leaving room for further investigations of these special cases.

We believe these demonstrative results, supported by a comprehensive set of Supporting Information (Gerighausen et al. 2024) downloadable at https://doi.org/10.5281/zenodo.12923703, will be of immediate and straightforward use to various experienced stakeholders, in for example the energy and health sectors, and provide a refined interpretation of the typical regime approach that will be of use to researchers of midlatitude dynamics. The consideration of regime projections as an additional source of information within an already adopted regime framework provides a complementary perspective to the hierarchical weather type/weather regime approach operationalized by the UK Met Office (Neal et al. 2016, 2024), and both will have relevance for different use cases. We note that for short-term (0–5 days) forecasting, when daily weather variability matters most for a local forecast, synoptic weather types might still be the first choice for a simplification of the weather situation. The regime framework is particularly suited for forecasts beyond 7 days, when forecast uncertainty increases.

In particular, continuous precursor indices may prove convenient and valuable low-dimensional inputs into data-driven forecast-calibration systems. Further work should aim to quantify the forecast skill and predictive power of the reanalysis-based results we present here. If we conceive of the multi-scale challenges of weather forecasting as requiring a 'hierarchy of data-analysis' just as we acknowledge the value of a hierarchy of computational models, then the approach we describe provides a valuable middle ground between a detailed (and data-intensive) consideration of the full atmospheric flow, combined weather-type–weather regime approaches, and a simple regime-mean framework. We are currently working toward a free provision of the proposed regime forecasts for enabling operational use.

Author Contributions

Judith Gerighausen: investigation, visualization, writing – original draft, writing – review and editing, software, data curation. **Joshua Oldham-Dorrington:** conceptualization, methodology, validation, supervision, software, data curation, writing – review and editing. **Fabian Mockert:** visualization, writing – review and editing, data curation. **Marisol Osman:** writing – review and editing, conceptualization, methodology, software, data curation, supervision, validation, visualization. **Christian M. Grams:** funding acquisition, writing – review and editing, validation, methodology, conceptualization, supervision, project administration, resources.

Acknowledgments

The contribution of J.D. and C.M.G. was partially embedded in the subprojects A8 and T2 of the Transregional Collaborative Research Center SFB/TRR 165 'Waves to Weather' (https://www.wavestoweather.de) funded by the Deutsche Forschungsgemeinschaft (DFG). The contribution of M.O. was supported by Axpo Solutions AG. C.M.G. acknowledges funding by the Helmholtz Association as part of the Young Investigator Group "Sub-seasonal Predictability: Understanding the Role of Diabatic Outflow" (SPREADOUT, grant VH-NG-1243). We thank Christopher Polster (Waves to Weather subproject A8 at University of Mainz) for providing the Flottplot package used in the Supporting Information.

We thank the authors of the python package "regionmask" for providing code via https://github.com/regionmask/regionmask used for country aggregation. Open Access funding enabled and organized by Projekt DEAL.

Conflicts of Interest

The authors declare no conflicts of interest.

Data Availability Statement

The data that support the findings of this study are openly available in an online figure repository at https://zenodo.org/records/12923703.

References

Baldwin, M. P., D. B. Stephenson, D. W. J. Thompson, T. J. Dunkerton, A. J. Charlton, and A. O'Neill. 2003. "Stratospheric Memory and Skill of Extended-Range Weather Forecasts." *Science* 301, no. 5633: 636–640. https://doi.org/10.1126/science.1087143.

Bieli, M., S. Pfahl, and H. Wernli. 2015. "A Lagrangian Investigation of Hot and Cold Temperature Extremes in Europe." *Quarterly Journal of the Royal Meteorological Society* 141, no. 686: 98–108. https://doi.org/10.1002/qj.2339.

Bloomfield, H. C., D. J. Brayshaw, and A. J. Charlton-Perez. 2020. "Characterizing the Winter Meteorological Drivers of the European Electricity System Using Targeted Circulation Types." *Meteorological Applications* 27, no. 1: e1858. https://doi.org/10.1002/met.1858.

Bloomfield, H. C., D. J. Brayshaw, P. L. M. Gonzalez, and A. Charlton-Perez. 2021. "Pattern-Based Conditioning Enhances Sub-Seasonal Prediction Skill of European National Energy Variables." *Meteorological Applications* 28, no. 4: e2018. https://doi.org/10.1002/met.2018.

Büeler, D., R. Beerli, H. Wernli, and C. M. Grams. 2020. "Stratospheric Influence on ECMWF Sub-Seasonal Forecast Skill for Energy-Industry-Relevant Surface Weather in European Countries." *Quarterly Journal of the Royal Meteorological Society* 146, no. 733: 3675–3694. https://doi.org/10.1002/qj.3866.

Büeler, D., L. Ferranti, L. Magnusson, J. F. Quinting, and C. M. Grams. 2021. "Yearround Subseasonal Forecast Skill for Atlanticeuropean Weather Regimes." *Quarterly Journal of the Royal Meteorological Society* 147, no. 741: 4283–4309. https://doi.org/10.1002/qj.4178.

Buizza, R., and M. Leutbecher. 2015. "The Forecast Skill Horizon." *Quarterly Journal of the Royal Meteorological Society* 141, no. 693: 3366–3382. https://doi.org/10.1002/qj.2619.

Charney, J. G., and J. G. DeVore. 1979. "Multiple Flow Equilibria in the Atmosphere and Blocking." *Journal of the Atmospheric Sciences* 36, no. 7: 1205–1216. https://doi.org/10.1175/1520-0469(1979)036<1205:MFEITA>2.0.CO;2.

Domeisen, D. I. V., A. H. Butler, A. J. Charlton-Perez, et al. 2020. "The Role of the Stratosphere in Subseasonal to Seasonal Prediction: 2. Predictability Arising From Stratosphere-Troposphere Coupling." *Journal of Geophysical Research: Atmospheres* 125, no. 2: e2019JD030923. https://doi.org/10.1029/2019JD030923.

Faranda, D., G. Masato, N. Moloney, et al. 2016. "The Switching Between Zonal and Blocked Mid-Latitude Atmospheric Circulation: A Dynamical System Perspective." *Climate Dynamics* 47, no. 5: 1587–1599. https://doi.org/10.1007/s00382-015-2921-6.

Ferranti, L., S. Corti, and M. Janousek. 2015. "Flow-Dependent Verification of the Ecmwf Ensemble Over the Euro-Atlantic Sector." *Quarterly Journal of the Royal Meteorological Society* 141, no. 688: 916–924. https://doi.org/10.1002/qj.2411.

Gerighausen, J., J. Dorrington, M. Osman, and C. M. Grams. 2024. *Collection of Figures to Explore Intra-Regime Weather Variability of North Atlantic-European Year-Round Weather Regimes as Supplementary Dataset for Gerighausen et al*. Technical Reports. Zenodo Repository. https://doi.org/10.5281/zenodo.12923703.

Grams, C. M., R. Beerli, S. Pfenninger, I. Staffell, and H. Wernli. 2017. "Balancing Europes Wind-Power Output Through Spatial Deployment Informed by Weather Regimes." *Nature Climate Change* 7, no. 8: 557–562. https://doi.org/10.1038/nclimate3338.

Grams, C. M., L. Magnusson, and L. Ferranti. 2020. "How to Make Use of Weather Regimes in Extended-Range Predictions for Europe." *ECMWF Newsletter* 2020, no. 165: 14–19.

Hannachi, A., D. M. Straus, C. L. E. Franzke, S. Corti, and T. Woollings. 2017. "Low-Frequency Nonlinearity and Regime Behavior in the Northern Hemisphere Extratropical Atmosphere." *Reviews of Geophysics* 55, no. 1: 199–234. https://doi.org/10.1002/2015RG000509.

Harrison, S. R., J. O. Pope, R. A. Neal, F. K. Garry, R. Kurashina, and D. Suri. 2022. "Identifying Weather Patterns Associated With Increased Volcanic Ash Risk Within British Isles Airspace." *Weather and Forecasting* 37, no. 7: 1157–1168. https://doi.org/10.1175/WAF-D-22-0023.1.

Hauser, S., S. Mueller, X. Chen, T.-C. Chen, J. G. Pinto, and C. M. Grams. 2023. "The Linkage of Serial Cyclone Clustering in Western Europe and Weather Regimes in the North Atlantic-European Region in Boreal Winter." *Geophysical Research Letters* 50, no. 2: e2022GL101900. https://doi.org/10.1029/2022GL101900.

Hauser, S., F. Teubler, M. Riemer, P. Knippertz, and C. M. Grams. 2023. "Towards a Holistic Understanding of Blocked Regime Dynamics Through a Combination of Complementary Diagnostic Perspectives." *Weather and Climate Dynamics* 4, no. 2: 399–425. https://doi.org/10.5194/wcd-4-399-2023.

Hersbach, H., B. Bell, P. Berrisford, et al. 2020. "The ERA5 Global Reanalysis." *Quarterly Journal of the Royal Meteorological Society* 146, no. 730: 1999–2049. https://doi.org/10.1002/qj.3803.

Hess, P., and H. Brezowsky. 1952. "Katalog der grosswetterlagen europas." In *Berichte des Deutschen Wetterdienstes in der US-Zone*, vol. 33. Dt. Wetterdienst.

Hess, P., and H. Brezowsky. 1977. "Katalog der grosswetterlagen europas 1881–1976, 3. verbesserte und ergänzte auflage." In *Berichte des Deutschen Wetterdienstes in der US-Zone*, 113. Deutscher Wetterdienst.

Hochman, A., G. Messori, J. F. Quinting, J. G. Pinto, and C. M. Grams. 2021. "Do Atlantic-European Weather Regimes Physically Exist?" *Geophysical Research Letters* 48, no. 20: e2021GL095574. https://doi.org/10.1029/2021GL095574.

Howard, E., S. Thomas, T. H. Frame, et al. 2022. "Weather Patterns in Southeast Asia: Relationship With Tropical Variability and Heavy Precipitation." *Quarterly Journal of the Royal Meteorological Society* 148, no. 743: 747–769. https://doi.org/10.1002/qj.4227.

Lee, S. H., J. C. Furtado, and A. J. Charlton-Perez. 2019. "Wintertime North American Weather Regimes and the Arctic Stratospheric Polar Vortex." *Geophysical Research Letters* 46, no. 24: 14892–14900. https://doi.org/10.1029/2019GL085592.

Lee, S. H., M. K. Tippett, and L. M. Polvani. 2023. "A New Year-Round Weather Regime Classification for North America." *Journal of Climate* 1: 1–42. https://doi.org/10.1175/JCLI-D-23-0214.1.

Liu, Y., S. Feng, Y. Qian, H. Huang, and L. K. Berg. 2023. "How Do North American Weather Regimes Drive Wind Energy at the Sub-Seasonal to Seasonal Timescales?" *Npj Climate and Atmospheric Science* 6, no. 1: 100. https://doi.org/10.1038/s41612-023-00403-5.

Matsueda, M., and M. Kyouda. 2016. "Wintertime East Asian Flow Patterns and Their Predictability on Medium-Range Timescales."

Scientific Online Letters on the Atmosphere 12: 121–126. https://doi.org/10.2151/sola.2016-027.

Matsueda, M., and T. N. Palmer. 2018. "Estimates of Flowdependent Predictability of Wintertime Euroatlantic Weather Regimes in Mediumrange Forecasts." *Quarterly Journal of the Royal Meteorological Society* 144, no. 713: 1012–1027. https://doi.org/10.1002/qj.3265.

Messori, G., and J. Dorrington. 2023. "A Joint Perspective on North American and Euro-Atlantic Weather Regimes." *Geophysical Research Letters* 50, no. 21: e2023GL104696. https://doi.org/10.1029/2023GL104696.

Michelangeli, P.-A., R. Vautard, and B. Legras. 1995. "Weather Regimes: Recurrence and Quasi Stationarity." *Journal of the Atmospheric Sciences* 52, no. 8: 1237–1256. https://doi.org/10.1175/1520-0469(1995)052<1237:WRRAQS>2.0.CO;2.

Mockert, F., C. M. Grams, T. Brown, and F. Neumann. 2023. "Meteorological Conditions During Periods of Low Wind Speed and Insolation in Germany: The Role of Weather Regimes." *Meteorological Applications* 30, no. 4: e2141. https://doi.org/10.1002/met.2141.

Neal, R., D. Fereday, R. Crocker, and R. E. Comer. 2016. "A Flexible Approach to Defining Weather Patterns and Their Application in Weather Forecasting Over Europe." *Meteorological Applications* 23, no. 3: 389–400. https://doi.org/10.1002/met.1563.

Neal, R., J. Robbins, R. Crocker, et al. 2024. "A Seamless Blended Multi-Model Ensemble Approach to Probabilistic Medium-Range Weather Pattern Forecasts Over the UK." *Meteorological Applications* 31, no. 1: e2179. https://doi.org/10.1002/met.2179.

Osman, M., R. Beerli, D. Büeler, and C. M. Grams. 2023. "Multimodel Assessment of Subseasonal Predictive Skill for Yearround Atlanticeuropean Weather Regimes." *Quarterly Journal of the Royal Meteorological Society* 149, no. 755: 2386–2408. https://doi.org/10.1002/qj.4512.

Reinhold, B. B. 1987. "Weather Regimes: The Challenge in Extended-Range Forecasting." *Science* 235, no. 4787: 437–441. https://doi.org/10.1126/science.235.4787.437.

Reinhold, B. B., and R. T. Pierrehumbert. 1982. "Dynamics of Weather Regimes: Quasi-Stationary Waves and Blocking." *Monthly Weather Review* 110, no. 9: 1105–1145. https://doi.org/10.1175/1520-0493(1982)110<1105:DOWRQS>2.0.CO;2.

Richardson, D., R. Neal, R. Dankers, et al. 2020. "Linking Weather Patterns to Regional Extreme Precipitation for Highlighting Potential Flood Events in Medium- to Long-Range Forecasts." *Meteorological Applications* 27, no. 4: e1931. https://doi.org/10.1002/met.1931.

Schiemann, R., and C. Frei. 2010. "How to Quantify the Resolution of Surface Climate by Circulation Types: An Example for Alpine Precipitation." *Physics and Chemistry of the Earth, Parts A/B/C* 35, no. 9–12: 403–410. https://doi.org/10.1016/j.pce.2009.09.005.

Souto, L., R. Neal, J. O. Pope, P. L. M. Gonzalez, J. Wilkinson, and P. C. Taylor. 2024. "Identification of Weather Patterns and Transitions Likely to Cause Power Outages in the United Kingdom." *Communications Earth & Environment* 5, no. 1: 1–10. https://doi.org/10.1038/s43247-024-01217-w.

Spaeth, J., P. Rupp, M. Osman, C. M. Grams, and T. Birner. 2024. "Flowdependence of Ensemble Spread of Subseasonal Forecasts Explored via North Atlantic-European Weather Regimes." *Geophysical Research Letters* 51, no. 14: e2024GL109733. https://doi.org/10.1029/2024GL109733.

Stephens, M. A. 1974. "Edf Statistics for Goodness of Fit and Some Comparisons." *Journal of the American Statistical Association* 69, no. 347: 730–737. https://doi.org/10.1080/01621459.1974.10480196.

Tveito, O. E., and R. Huth. 2016. "Circulation-Type Classifications in Europe: Results of the COST 733 Action." *International Journal of Climatology* 36, no. 7: 2671–2672. https://doi.org/10.1002/joc.4768.

Van Der Wiel, K., H. C. Bloomfield, R. W. Lee, et al. 2019. "The Influence of Weather Regimes on European Renewable Energy Production and Demand." *Environmental Research Letters* 14, no. 9: 94010. https://doi.org/10.1088/1748-9326/ab38d3.

Vautard, R. 1990. "Multiple Weather Regimes Over the North Atlantic: Analysis of Precursors and Successors." *Monthly Weather Review* 118, no. 10: 2056–2081. https://doi.org/10.1175/1520-0493(1990)118<2056:MWROTN>2.0.CO;2.

Yiou, P., and M. Nogaj. 2004. "Extreme Climatic Events and Weather Regimes Over the North Atlantic: When and Where?" *Geophysical Research Letters* 31, no. 7. https://doi.org/10.1029/2003GL019119.

Zubiate, L., F. McDermott, C. Sweeney, and M. O'Malley. 2017. "Spatial Variability in Winter NAO–Wind Speed Relationships in Western Europe Linked to Concomitant States of the East Atlantic and Scandinavian Patterns." *Quarterly Journal of the Royal Meteorological Society* 143, no. 702: 552–562. https://doi.org/10.1002/qj.2943.

Supporting Information

Additional supporting information can be found online in the Supporting Information section. **Data S1:** Supporting Information.